Systole Length and Preservation Under Belt-Sums of the Borromean Rings

Amanda Cowell

August 17, 2018

Abstract

Through the use of Mobius transformations, we establish gluing maps for the fundamental polyhedron of the complement of the Borromean rings Ω. We then use these transformations to describe curves with base point x_0 belonging to the fundamental group of Ω, denoted $\pi_1(\Omega, x_0)$. Taking the quotient space (reducing the set of curves to the equivalence classes) we locate which curves have systolic length of $\ell = 2.12255$. From here, we identify relevant thrice-punctured spheres S and determine the existence of a systole living in $\Omega \setminus S$ for each of case of these thrice-punctured spheres. Finally, we uncover why a particular type of manifold with no curve of length ℓ must not include the Borromean rings belt-summand.

1 Borromean Rings

A *knot* is a closed curve in three dimensions, whereas a *link* is a collection of knots that can be intertwined. One way to study a link L is through the link complement $S^3 \setminus L$, where S^3 is the unit sphere in $\mathbb{R}^4$. Alternatively, this can be thought of as $\mathbb{R}^3 \cup \{\infty\}$. A *hyperbolic link* is a link such that the complement can be described as a complete hyperbolic manifold.

The Borromean rings is a type of Brunnian link, meaning if any one of the three curves that make up the link are removed then the other two components are left disjoint. It is typically depicted with symmetry as in Figure 1, but can be isotoped to form Figure 2. The isotoped version will be the form of the Borromean rings we will use throughout this paper.

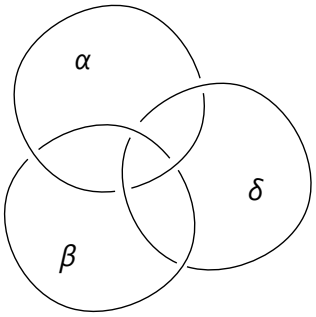

Figure 1: Borromean rings

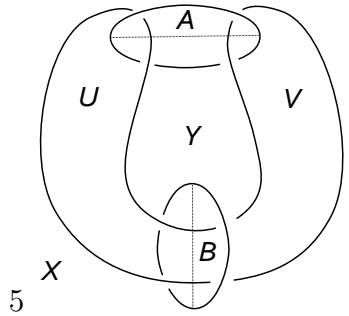

Figure 2: Borromean Rings Isotopy

In order to study the Borromean rings, we will first introduce the process of cell decomposition into the fundamental polyhedron. Begin by placing the Borromean rings on a plane such that the crossing discs A and B are perpendicular to that plane, as in Step 1 of Figure 3, where the dotted lines indicate the intersection of A, B with the plane. Let the portion above the plane be called P_+ and the portion below the plane be P_-. For a moment, consider only P_+, where we are dealing with the top half of the crossing discs, as pictured in Step 2 of Figure 3.

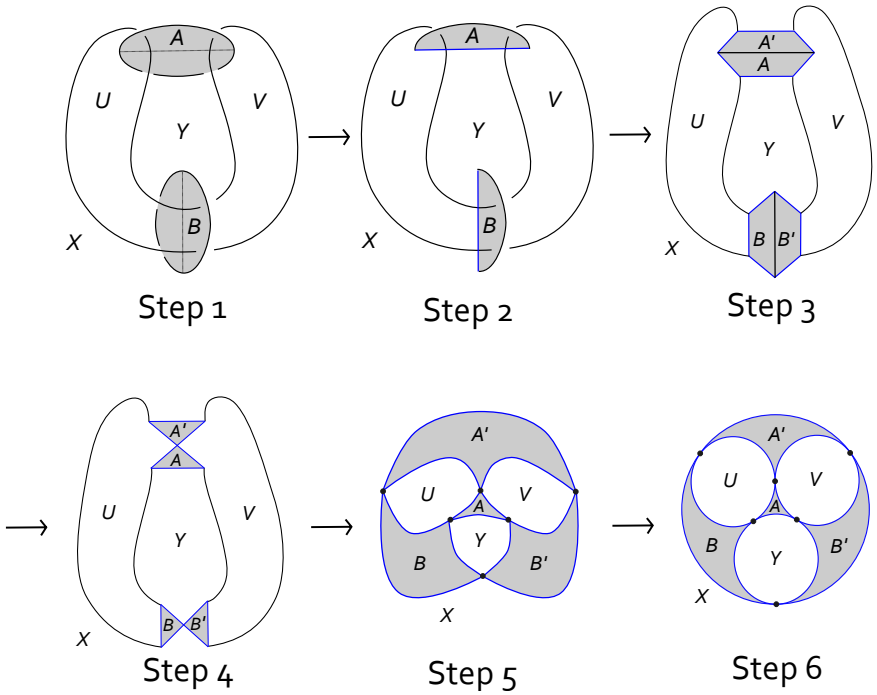

Figure 3: Decomposition Steps

Slice along the bottom of the semi-disc and open it up (similar to spreading a pita bread apart) in order to have a region representing the front and back of each disc. In Step 3 of Figure 3, we separate the front and back by stretching the straight edge apart, making

the crossing discs planar. The two link strands will still be attached to the edge, and the crossing circle strand will shrink, see Step 3 Figure 3. Isotopically make a triangle out of the three points by shrinking the crossing circle arc to a point and deforming the deforming the crossing disc regions, illustrated by Step 4 of Figure 3. Next, shrink the other link strands to points by deforming the crossing disc regions until they touch at these link points, Step 5 of Figure 3.

Now comes the circle packing, Step 6 of Figure 3, where we identify the regions between the crossing discs and deform them to a circle. The circles created will preserve tangencies to the other regions, including the outer circle corresponding to the infinite region outside of the link. The circle packing is a cell decomposition of the boundary of P_+, and we will have a reflection of this to represent the region below the plane in P_-. Since the *nerve* of the circle packing is K_4 (aka placing a dot in the center of each unshaded region and connecting said dots produces a structure where each vertex has three edges), we can see that the structure is *octahedral*, with P_+ and P_- as the two tetrahedrons that together make up the octahedron.

Once the steps are complete for the crossing discs, we can then take the circle packing and put it in hyperbolic 3-space, using the *upper-half space model*. In this model, as points get closer to the xy-plane, called the *ideal plane*, they actually become infinitely far away. Any point actually on the ideal plane is a point at infinity. We will also note that the shortest distance between any two points in hyperbolic geometry is a semi-circle. For purposes of studying the complement of the Borromean rings, we will put the link itself at infinity. By doing this, we take all of the points that make up the link in the circle packing from Figure 3 and place them at infinity. We will denote the complement of the Borromean rings by Ω, and since it is a hyperbolic structure, we can study it through hyperbolic geometry and the upper-half space model. Through this, we are able to study Ω and consequently, gain information about the hyperbolic structure on the Borromean rings.

At this point we have choices for which type of infinity we would like to utilize for the components of the Borromean rings, which correspond to the points of tangency in the circle packing. We will use the circle packing, Step 6 Figure 3, and choose the point σ in Figure 4 to be the point sent up to infinity, while all other points will be placed on the ideal plane. By symmetry of the Borromean rings, we can pick any point to be sent to infinity and get a similar structure. As σ is sent to infinity, the region Y opens up and B, B' become vertical faces, as depicted in Figure 4 Step 7, where the image on the left is a view looking down onto the ideal plane and the image on the right is an equivalent side view to give perspective. The next step in the process is to "shrinkwrap" Ω into hyperbolic space by keeping the points fixed and lifting the edges of the shaded regions so that these edges form semi-circles, which are lines in hyperbolic space. The shaded regions, A and A', then "balloon" up until they conform to a hemispheric shape. Step 8 of Figure 4 depicts a top-down view on the left and the perspective view on the right is shown with the vertical faces B, B' removed. The view looking down onto the floor provides a two-dimensional template for P_+ which we will combine with P_-, shown in Step 9, to learn more about Ω. Notice that P_- is a reflection of P_+ glued along Y. We will use the subscripts of $+$ and $-$ to indicate which part of the fundamental polyhedron each region belongs to.

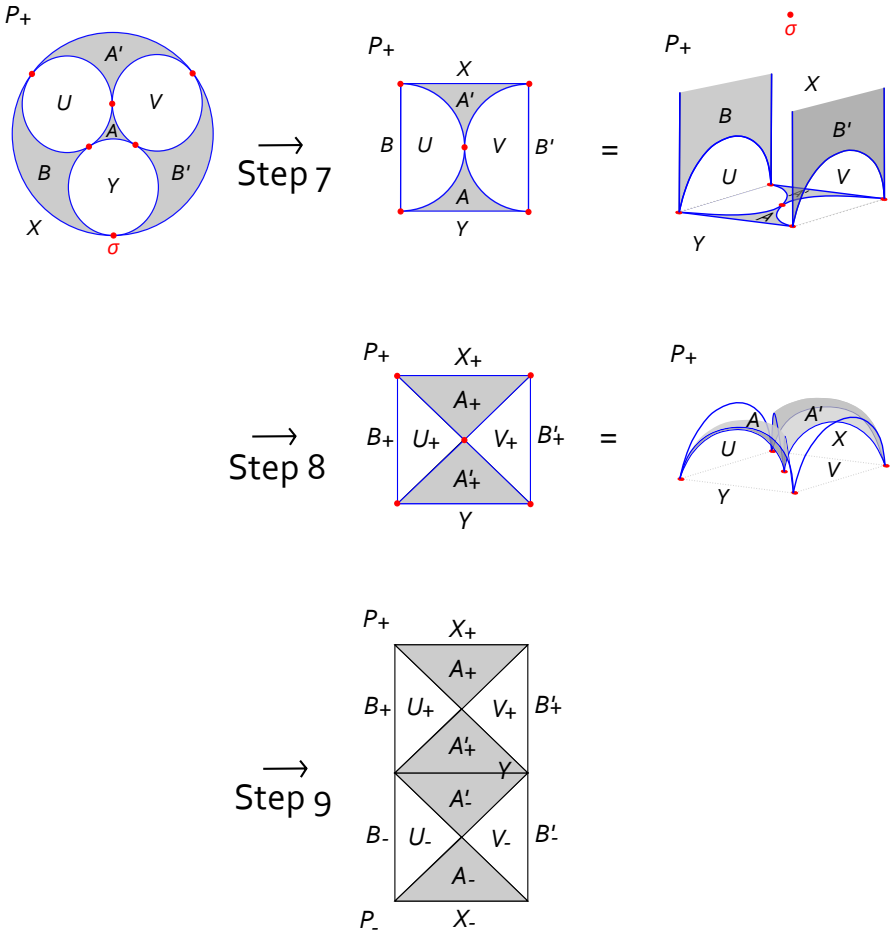

Figure 4: Fundamental Region steps

In order to explore the belt-sum operation (which we will introduce later), we first need to identify the possible thrice-punctured spheres in Ω that can be used during belt-summing. A *thrice-punctured sphere* is a sphere with three points removed. More information on thrice-punctured spheres can be found in *Thrice-Punctured Spheres in Hyperbolic 3-Manifolds* by Adams [1].

In Ω, there are only four cases of a thrice-punctured sphere that need to be considered [5]. By symmetry, we choose B to be one of the punctures to cover all possibilities. Moreover, the crossing circle B is at $\{\infty\}$, so any thrice-punctured sphere touching B appears as a plane in the fundamental region.

Case 1: The thrice-punctured sphere S_1 is punctured once by the longitude of the crossing circle B and twice by the link strands that run through the crossing disc B.

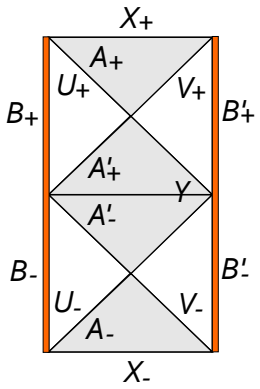

(a) S_1 on the Fundamental Polyhedron

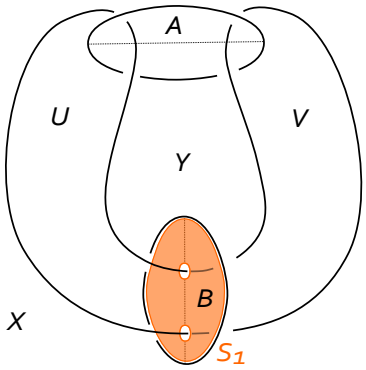

(b) S_1 in Ω

Figure 5: Case 1

Case 2: The thrice-punctured sphere S_2 is punctured once by the longitude of the crossing circle B and twice by the meridians of the crossing circle A.

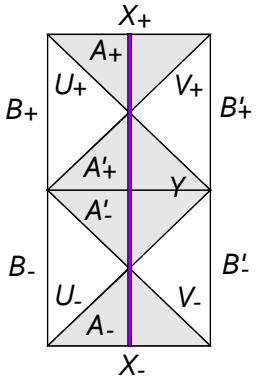

(a) S_2 on the Fundamental Polyhedron

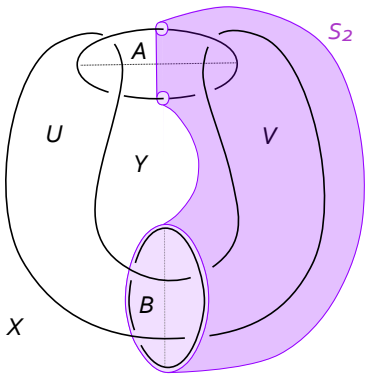

(b) S_2 in Ω

Figure 6: Case 2

Case 3: The thrice-punctured sphere S_3 is punctured twice by meridians of the crossing circle B and once by the longitude of the crossing circle A. Note that the shape of S_3 is "hollow" on the inside.

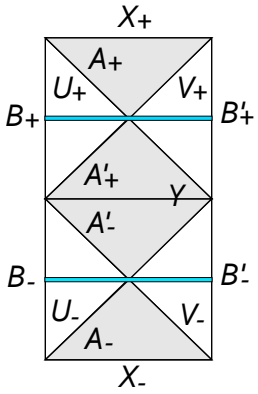

(a) S_3 on the Fundamental Polyhedron

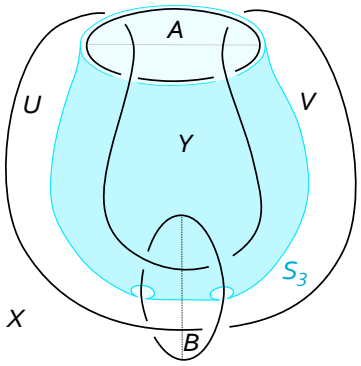

(b) S_3 in Ω

Figure 7: Case 3

Case 4: The thrice-punctured sphere S_4 is planar and punctured twice by meridians of the crossing circle B and once by the knot circle boundary $U \cup V$.

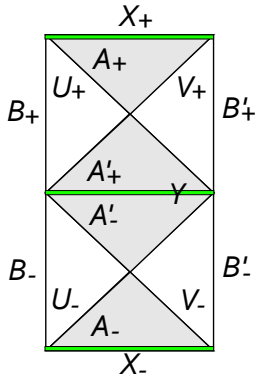

(a) S_4 on the Fundamental Polyhedron

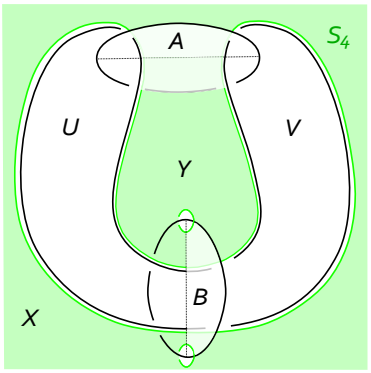

(b) S_3 in Ω

Figure 8: Case 4

2 The Fundamental Group of Ω

Consider a point x_0 placed anywhere in Ω as the base of a closed curve. Such a curve would begin at x_0, travel through the space and loop back to x_0. In this way, there are infinitely many ways such a loop could be drawn. Consider a curve such as α from Figure 9 which begins at x_0, wanders through Ω, and perhaps crossing itself a few times but never going

around any components of the Borromean rings. Despite any self-crossings or intertwining with another loop that also does not go around the Borromean rings, a curve such as α is considered homotopic to x_0, or *null-homotopic*, since there is no part of the actual link that prevents it from shrinking to a point. Notice that this type of loop differs from the other ones pictured in Figure 9. Curves that are NOT homotopic to a point are called *essential*, such as δ, β, and ε. It is important to note that these curves are strictly in the complement of the Borromean rings and are not an additional component of the link. Instead, these lines represent curves in Ω. Essential curves can be as simple as one loop around a strand such as β, or more complicated loops such as ε.

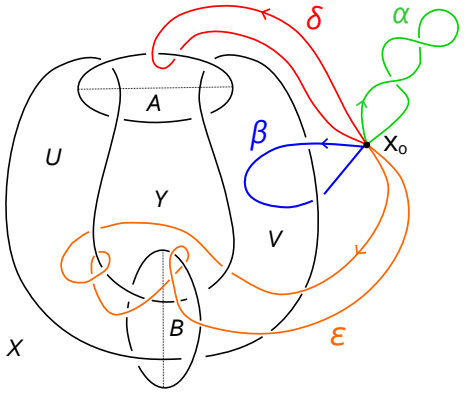

Figure 9: Curves in Ω

We will use λ to denote the set of all curves in Ω based at x_0. The set of curves based at x_0 in the quotient space $\lambda/_{homotopy}$ is called *the fundamental group of* Ω and denoted $\pi_1(\Omega, x_0)$. Since many curves are homotopic, it should be noted that the quotient space considers equivalence classes of curves in Ω. The fundamental group is useful as a tool to study the geometry behind this topological space by relating it to an algebraic structure. Given two curves $\delta, \beta \in \pi_1(\Omega, x_0)$, we can be multiply them to form a concatenation $\delta \circ \beta$. Multiplication in this group is not commutative so $\delta \circ \beta$ and $\beta \circ \delta$ will not give the same path once the operation is complete. Pictorially, multiplication can be completed by traveling along the first curve δ, then along the second curve β before going back to the initial point x_0, as seen in Figure 10.

Another important feature of the fundamental group is the fact that x_0 can be placed at any arbitrary point in Ω since every point is homotopic to every other point. The idea of fixing the base point is good convention for relaying information consistently, but the fixed base point can be removed to form free homotopy classes of Ω.

Simply describing these loops through pictures does not provide quite enough rigor to be super useful. Stating that curves can be "multiplied" appears questionable at this point, so we will introduce the notion of Möbius transformations as a way to describe these paths, and their multiplication, more precisely.

The fundamental polyhedron of the Borromean rings provides a convenient template to establish these curves through gluing maps. Beginning with the fundamental polyhedron,

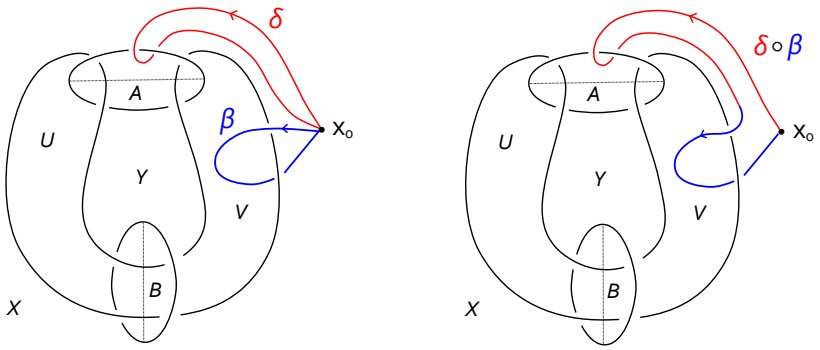

Figure 10: Multiplication of two curves $\delta \circ \beta$

we can work backward to say which regions will be glued back together to form the original shape. By placing the fundamental polyhedron on the complex plane, we can identify coordinates for each face and use a Möbius transformation to provide these gluing maps.

The general procedure begins with three points q, r, s on the target face and three corresponding points $\tilde{q}, \tilde{r}, \tilde{s}$ on the another face. By using the formula:

$$\frac{(z-q)(r-s)}{(z-s)(r-q)} = \frac{(w-\tilde{q})(\tilde{r}-\tilde{s})}{(z-\tilde{s})(\tilde{r}-\tilde{q})},$$

where z, w are variables coinciding to the input and output respectively, we can solve for w to obtain the transformation. The result will be of the form

$$w = \frac{az+b}{cz+d}$$

whose complex coefficients can be put in a matrix,

$$M = \begin{bmatrix} a & b \\ c & d \end{bmatrix}.$$

Let's make this idea a bit more concrete with an example. Say we want the map that glues A and A' in P_+ in Figure 11. We begin by placing the fundamental polyhedron on the complex plane and choose for the origin to be directly in the middle. Scale it so that it is 2 units wide and, consequently, 4 units in height (scaling preserves ratios). Then the region will have the coordinates as presented in Figure 11. By convention, we want A' to be glued to A making A' our target face, so we will first choose three points on A'. Namely let

$$q = -1 + 2i, r = i, \text{ and } s = 1 + 2i.$$

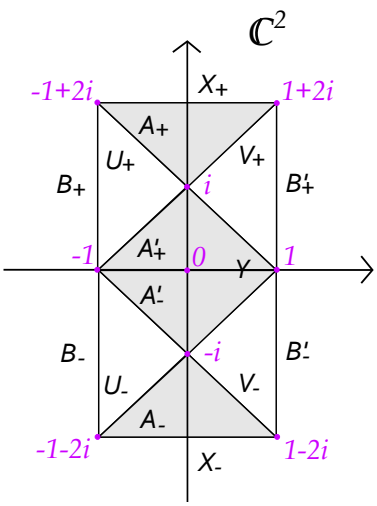

Figure 11: Fundamental Polyhedron on the Complex Plane

Keeping in mind where these points get glued back up to on A, we must find the three points on A that are identified with q, r, and s. Thus the corresponding points on A become

$$\tilde{q} = -1, \tilde{r} = i, \text{ and } \tilde{s} = 1.$$

Plugging these points into the formula, we obtain

$$\frac{(z+1-2i)(-1-i)}{(z-1-2i)(1-i)} = \frac{(w+1)(-1+i)}{(w-1)(1+i)}.$$

Solving for w produces

$$w = \frac{1}{z-2i},$$

where the matrix coefficients are $a = 0$, $b = 1$, $c = 1$, and $d = -2i$. Placing these in the matrix we get

$$M = \begin{bmatrix} 0 & 1 \\ 1 & -2i \end{bmatrix}.$$

In order for this matrix to be useful, the determinant must be equal to 1. Currently, it is not equal to 1 so we must normalize it by dividing by the square root of the determinant. Since $\det(M) = -1$, we divide each entry by i to get

$$M' = \begin{bmatrix} 0 & -i \\ -i & -2 \end{bmatrix}.$$

Notice that $\det(M') = 1$ and we are good to go! For clarity, we will name $M' = \varphi_{A_+}$ to indicate which faces are begin glued together. Repeating this process for each region being glued back together we obtain Table 1, which contains a consistent set of gluing maps for the Borromean rings.

Table 1: Table of Gluing Maps for the Borromean Rings

Map	Picture	Map	Picture
$\varphi_{A_+} : A_+ \to A'_+$ $\varphi_{A_+} = \begin{bmatrix} 0 & -i \\ -i & -2 \end{bmatrix}$	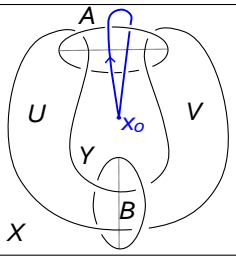	$\varphi^{-1}_{A_+} : A'_+ \to A_+$ $\varphi^{-1}_{A_+} = \begin{bmatrix} -2 & i \\ i & 0 \end{bmatrix}$	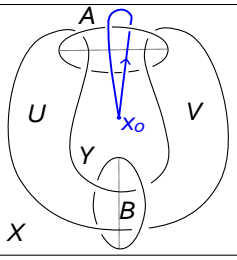
$\varphi_{A_-} : A_- \to A'_-$ $\varphi_{A_-} = \begin{bmatrix} -2 & -i \\ -i & 0 \end{bmatrix}$	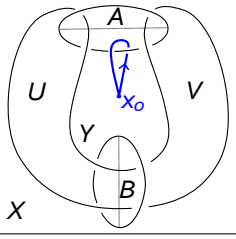	$\varphi^{-1}_{A_-} : A'_- \to A_-$ $\varphi^{-1}_{A_-} = \begin{bmatrix} 0 & i \\ i & -2 \end{bmatrix}$	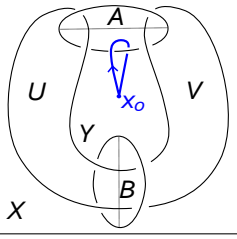
$\varphi_B : B \to B'$ $\varphi_B = \begin{bmatrix} 1 & 2 \\ 0 & 1 \end{bmatrix}$	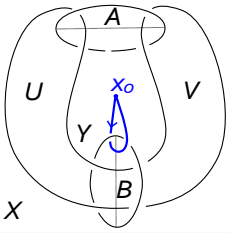	$\varphi^{-1}_B : B' \to B$ $\varphi^{-1}_B = \begin{bmatrix} 1 & -2 \\ 0 & 1 \end{bmatrix}$	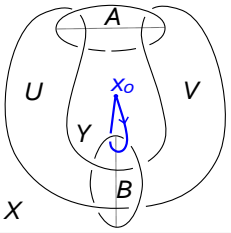
$\varphi_U : U_+ \to U_-$ $\varphi_U = \begin{bmatrix} 1-i & -i \\ i & 1+i \end{bmatrix}$	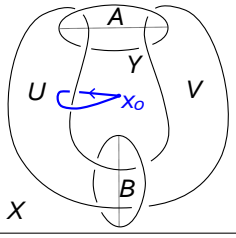	$\varphi^{-1}_U : U_- \to U_+$ $\varphi^{-1}_U = \begin{bmatrix} 1+i & i \\ -i & 1-i \end{bmatrix}$	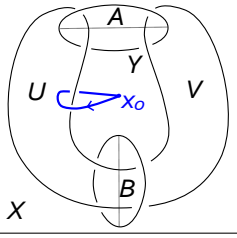
$\varphi_V : V_+ \to V_-$ $\varphi_V = \begin{bmatrix} i+1 & -i \\ i & 1-i \end{bmatrix}$	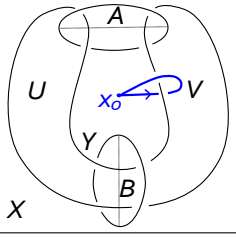	$\varphi^{-1}_V : V_- \to V_+$ $\varphi^{-1}_V = \begin{bmatrix} 1-i & i \\ -i & 1+i \end{bmatrix}$	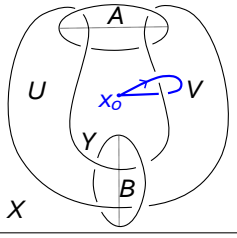
$\varphi_X : X_+ \to X_-$ $\varphi_X = \begin{bmatrix} 1 & 4i \\ 0 & 1 \end{bmatrix}$	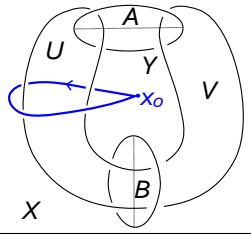	$\varphi^{-1}_X : X_- \to X_+$ $\varphi^{-1}_X = \begin{bmatrix} 1 & -4i \\ 0 & 1 \end{bmatrix}$	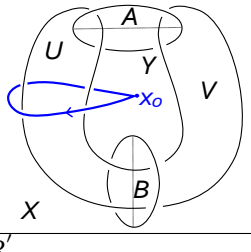
Note: $\varphi_B : B \to B' = \varphi_B : B_+ \to B'_+ = \varphi_B : B_- \mapsto B'_-$.			

Since all of these curves live in Ω (a hyperbolic manifold) we can compute the hyperbolic length. First, we must find the trace of the matrix of the gluing map, then using the hyperbolic length formula, $\ell = 2\text{arc}\cosh\left(\frac{\pm trace}{2}\right)$, we can compute the complex length of each curve.

For example, to find the length of the curve given by $\varphi_{A_+} : A_+ \to A'_+$ we first find the trace of the matrix, $trace(\varphi_{A_+}) = -2$. Then the complex length becomes $\ell_1 = 2\text{arc}\cosh\left(\frac{\pm(-2)}{2}\right) = 0$. This is expected as it is the length of a curve around a link strand, which can be shrunk as small as we like.

Let us consider a different curve that may seem a little less trivial. Suppose we want the length of a more interesting curve such as the one generated by $\varphi_{A_+} \circ \varphi_B$. We begin by multiplying the matrices,

$$\varphi_{A_+} \circ \varphi_B = \begin{bmatrix} 0 & -i \\ -i & -2 \end{bmatrix} \begin{bmatrix} 1 & 2 \\ 0 & 1 \end{bmatrix} = \begin{bmatrix} 0 & -i \\ -i & -2-2i \end{bmatrix}.$$

Next, we take $trace(\varphi_{A_+} \circ \varphi_B) = -2 - 2i$ and use the hyperbolic length formula to get $\ell_2 = 2.12255 + 1.80911i$. Notice that the result is a complex number where the real part is the real length and the imaginary part corresponds to the angle of rotation.

Using SnapPy, we found the *length spectum* of Ω, which are the lengths of all the curves, including multiplicity. The curves of most interest are the ones of shortest (real) length, called the *systole*. SnapPy found the systolic length, which was in fact $\ell = 2.12255$, meaning the curve $\varphi_{A_+} \circ \varphi_B$ must be one of our systoles.

By multiplying all possible combinations of matrices from Table 1 above, we found many curves of systolic length. We also determined many of these combinations actually correspond to the same curve. Using this information, we noticed the following:

Lemma 2.1. *If $S \subset \Omega$ is a thrice-punctured sphere, then there exists a systole in $\Omega \setminus S$.*

Proof. Let S be a thrice-punctured sphere in Ω. By symmetry, we can assume the crossing circle B is where one of the punctures occur. By Ransom [5], there are four possible cases; these are illustrated in Figures 5-8.

In Case 1, an example of a systole that does not intersect the corresponding thrice-punctured sphere S_1 from Figure 5 can be described by the composition of Möbius transformations $\varphi_{A_+} \circ \varphi_V$, as seen in Figure 12a. This sphere S_1 is punctured once by the crossing circle B and twice by the strands that go through the middle of the crossing disc B. The systole $\varphi_{A_+} \circ \varphi_V$ starts at the point x_0, first traveling through the backside of the crossing disc A_+ to the front, next through the bottom of the region V, coming out the top of V, then finally back to the point x_0. This geodesic representative which lives in $\Omega \setminus S_1$ has the systole length of $\ell = 2.12255$ and does not intersect S_1, thus exists in $\Omega \setminus S_1$.

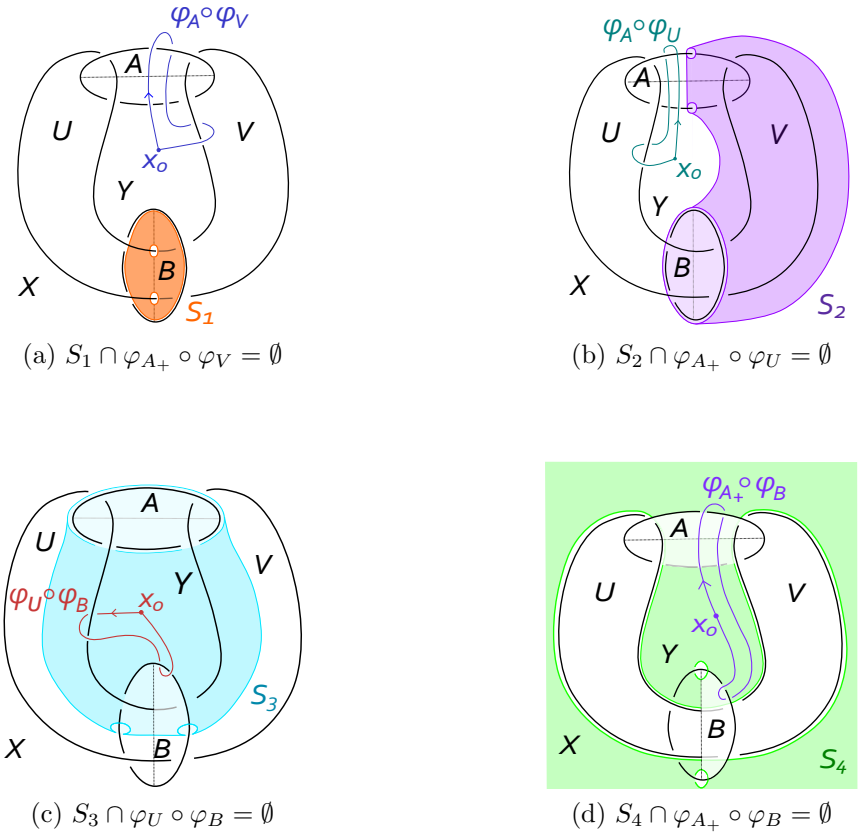

(a) $S_1 \cap \varphi_{A_+} \circ \varphi_V = \emptyset$ (b) $S_2 \cap \varphi_{A_+} \circ \varphi_U = \emptyset$

(c) $S_3 \cap \varphi_U \circ \varphi_B = \emptyset$ (d) $S_4 \cap \varphi_{A_+} \circ \varphi_B = \emptyset$

Figure 12: Thrice-punctured spheres and the corresponding disjoint systole.

An example of a systole that does not intersect the thrice-punctured sphere S_2 from Case 2, Figure 6, can be described by the composition of Möbius transformations $\varphi_{A_+} \circ \varphi_U$. Together, these can be in Figure 12b. Here, the sphere S_3 has three punctures given by meridians of the crossing circle A in P_+ and P_-, as well as longitude around the outside of the crossing disc B. A systole that misses the manifold S_2 is described by $\varphi_{A_+} \circ \varphi_U$. This simple closed geodesic begins at x_0, travels through the backside of A_+ then through the bottom of U, through P_- to P_+, and back to x_0. By going through the part of the crossing disc A_+ that is not contained in the thrice-punctured sphere, and through the region U (which does not intersect S_2) this curve never intersects the thrice-punctured sphere S_2. This geodesic representative has the systole length of $\ell = 2.12255$ and is a systole existing in $\Omega \setminus S_2$.

It should be noted that the thrice-punctured sphere that is the vertical reflection of S_2 has the same punctures and is symmetric to the case shown here. In this situation, the sphere would surround the region U and the systole will go through the region V instead of U, using the Möbius transformation $\varphi_{A_+} \circ \varphi_V$.

The third instance of a thrice-punctured sphere comes from Case 3, Figure 7, where the systole of interest can be described by the composition of Möbius transformations $\varphi_U \circ \varphi_B$, pictured in Figure 12c. The sphere S_3 is "empty" on the inside; that is, its shape is more

like a sock with a couple of toe holes, and the parts of the Borromean rings that appear to be covered by the sphere S_3 are actually in the hollow of the manifold. The systole in this instance is described by $\varphi_U \circ \varphi_B$, which is also in the vacant space. This geodesic begins at x_0, moves through the bottom of the region U to the top of U, through the front of B_+, and back to x_0. This geodesic representative has the systole length of $\ell = 2.12255$ and does not intersect the thrice-punctured sphere, thus exists entirely in $\Omega \setminus S_3$.

In Case 4, Figure 8, an example of a systole that does not intersect the corresponding thrice-punctured sphere can be described by the composition of Möbius transformations $\varphi_{A_+} \circ \varphi_B$, as seen in Figure 12d. The thrice-punctured sphere S_4 is the union of the regions X and Y, and thus is planar. The crossing discs A and B are perpendicular to the plane, and each only intersects $X \cup Y$ in a line. Hence the simple closed geodesic described by $\varphi_{A_+} \circ \varphi_B$ is entirely above the plane in P_+ and does not intersect the thrice-punctured sphere at any point. This geodesic representative has complex length of $\ell = 2.12255$ and thus is a systole existing in $\Omega \setminus S_4$.

Therefore, no matter which thrice-punctured sphere $S \subset \Omega$, there exists a a systole that is entirely within $\Omega \setminus S$. □

3 Belt Sums

The belt-sum operation has been studied for its ability to retain volume when dealing with specific types of hyperbolic 3-manifolds. The belt-sum method begins by cutting particular orientable finite volume hyperbolic 3-manifolds along totally geodesic incompressible thrice-punctured spheres, then regluing two copies of each thrice-punctured sphere by a particular isometry [1]. A *cusp* is topologically a tubular neighborhood of the link intersected with the link complement [2].

It is remarkable that once a belt-sum is done properly, the volume stays the same. Another extraordinary fact that follows is the preservation of certain curves in the complement. Since the operation only requires slicing along the thrice-punctured sphere, curves disjoint from said sphere get carried along and retain certain properties. From this, we deduce the following theorem.

Theorem 3.1. *If M is a hyperbolic 3-manifold with cusps whose length spectrum does not include a curve of length $\ell = 2.12255$ then M does not include a Borromean rings belt-summand.*

Proof. Consider the complement of the Borromean rings Ω and some other hyperbolic manifold M'. In order to create a belt sum, begin by locating a thrice-punctured sphere $S_\Omega \subset \Omega$ and a thrice-punctured sphere $S_{M'} \subset M'$. Slice along each of the spheres and glue corresponding components of them, being sure to join the copies of S_Ω to those of $S_{M'}$. Any curves in Ω that do not intersect S_Ω will be preserved once the belt sum is complete, as well as any curves in M' that do not intersect $S_{M'}$. By Lemma 2.1, it is clear that there exists a curve of length $\ell = 2.12255$ that does not get cut no matter which thrice-punctured sphere

in Ω is sliced during belt summing. Therefore, any belt-summand that includes at least one copy of the Borromean rings will result in at least one curve with length $\ell = 2.12255$. $\square$

4 Open Questions

- How does the length spectrum behave under belt-sums?
- Can a similar process be extended to other classes of links?
- Which curves live on totally geodesic surfaces?
- Is there a relationship between the length spectrum of the Whitehead link and the Borromean rings?

5 Acknowledgments

An enormous thanks goes to my advisor, Rolland Trapp. I would also like to thank the NSF and CSUSB for their generous support, as well as Corey Dunn for his role in the REU program. This research was funded under NSF grant number 1758020.

References

[1] C. Adams
Thrice-Punctured Spheres in Hyperbolic 3-Manifolds,
Transactions of the American Mathematical Society 287, no. 2, pp. 645–656 (1985).

[2] C. Adams, R. Kaplan-Kelly, M. Moore, B. Shapiro, S. Sridhar, J. Wakefield
Densities of Hyperbolic Cusp Invariants,
arXiv:1701.03479 (2017).

[3] W. S. Massey
Algebraic Topology: An Introduction,
Springer-Verlag, Berlin (1967).

[4] T. Needham
Visual Complex Analysis,
Clarendon Press, Oxford (1997).

[5] B. Ransom
Factorization of Fully Augmented Links via Belted Sum Decomposition
CSUSB REU (2018).